

Correlation between stiffener configurations and load capacity for pipe support beam

Tsaqif Al Farrel Ghazali ^{1*}, Mohd Shukri Yob ^{1*},
Mohd Juzaila Abd Latif ², Ojo Kurdi ³, Fudhail Abdul Munir ⁴

¹ Applied Mechanical Design Laboratory, Universiti Teknikal Malaysia Melaka, Melaka, 76100, Malaysia

² Faculty of Mechanical Technology and Engineering, Universiti Teknikal Malaysia Melaka, Melaka, 76100, Malaysia

³ Department of Mechanical Engineering, Diponegoro University, Semarang, 50275, Indonesia

⁴ Department of Mechanical Engineering, Universiti Teknologi Petronas, Perak, 32610, Malaysia

ABSTRACT

Pipe supports play a critical role in ensuring the safe operation of piping systems in industrial environments. When additional piping is introduced, these supports must be reinforced to accommodate increased loads. This study investigates the influence of stiffener parameters, there are beam size, stiffener distance, and stiffener thickness on the load capacity of pipe supports using both experimental testing and finite element analysis (FEA). A stiffened pipe support model was developed and subjected to concentrated load testing, and the corresponding FEA model was validated against the experimental results, achieving an average accuracy of 94.62%. The findings indicate that beam size significantly affects load capacity, while stiffener distance has a more pronounced effect in medium to large beams. In contrast, variations in stiffener thickness showed minimal impact. These results provide valuable insights for engineers aiming to optimize pipe support configurations and establish a foundation for design optimization in manufacturing applications.

Keywords: Load capacity, Stiffener, Pipe support, Finite element analysis.

OPEN ACCESS

Received: July 28, 2025

Revised: October 11, 2025

Accepted: December 10, 2025

Corresponding Author:

Tsaqif Al Farrel Ghazali
al.farrel.ghazali16@gmail.com
Mohd Shukri Yob
mshukriy@utem.edu.my

 **Copyright:** The Author(s).

This is an open-access article distributed under the terms of the [Creative Commons Attribution License \(CC BY 4.0\)](https://creativecommons.org/licenses/by/4.0/), which permits unrestricted distribution provided the original author and source are cited.

Publisher:

[Chaoyang University of Technology](https://www.chaoyang.edu.my/)

ISSN: 1727-2394 (Print)

ISSN: 1727-7841 (Online)

1. INTRODUCTION

Piping systems are essential for transporting various fluids to storage or processing areas across many industries. These systems can be installed either directly on the ground or on elevated structures. Ground installations, however, often present accessibility challenges during maintenance operations. To overcome these limitations, elevated structures—commonly referred to as pipe supports—are employed, allowing for more efficient use of space and improved accessibility (Nagdeote et al., 2021).

Pipe supports serve the primary function of holding multiple pipes that carry different liquids or gases during operation (Drake and Walter, 2010). In addition to supporting pipes, these structures may also bear mechanical and electrical components connected to the piping system (Meshram and Prasad, 2021; Kurepatil et al., 2024). As such, it is essential to ensure the continuous and safe operation of these systems to prevent production interruptions (Kawade and Navale, 2019).

In certain cases, the introduction of new pipelines increases the loading demands on existing pipe supports. Two common strategies are available to increase load capacity: utilizing a larger beam or incorporating stiffeners. While replacing a beam with a larger one is effective, it involves high costs and complex modification processes. Alternatively, stiffeners can be added to enhance load capacity. This approach is widely adopted due to its ease of fabrication and ability to improve structural rigidity without significantly increasing weight (Alinia, 2005; Sinur and Beg, 2012; Bougoffa et al., 2023; Wang and Zhang, 2023; Huang et al., 2024; Lee et al., 2024).

Finite Element Analysis (FEA) has become a widely used method for predicting stress in structural components (Chen and Ou, 2009; Alshoabi, 2015; Gupta et al., 2022; Shah and Ganesh, 2022). Its advantages have enabled researchers to perform extensive stress analysis, particularly on beams reinforced with stiffeners, to evaluate their load capacities (Maiorana et al., 2011; Gavare and Patil, 2018; Basiński, 2019; Papazafeiropoulos et al., 2022; Bougoffa et al., 2023; Peng et al., 2023).

However, conducting FEA requires specialized knowledge and a range of design decisions (Plevris and Markeset, 2018; Nerenst et al., 2021). Despite the availability of academic guidelines, FEA implementation in industry remains limited (Nerenst et al., 2021). One key challenge is the lack of standardized guidelines for defining stiffener parameters such as geometry, placement, and distance (Choi et al., 2007; Sholikhah et al., 2024; Zhang et al., 2024). This absence complicates fabrication and hinders practical application. Therefore, further research is required to establish practical design recommendations that address these challenges and assist engineers during construction (Tsavdaridis and Galiatsatos, 2015; Wang and Zhang, 2023).

This study aims to establish a correlation between stiffener configurations and the load capacity of pipe support beams. Both experimental testing and finite element simulations were performed. The findings are intended to serve as a guideline for engineers in selecting optimal stiffener configurations for pipe support applications.

2. CONCENTRATED LOAD TESTING

2.1 Geometry of Pipe Support with Stiffener Reinforcement

The pipe support model with stiffener reinforcement, as illustrated in Fig. 1, consists of a vertical column and a reinforced horizontal beam. This model of pipe support was chosen according to Yussof et al. (2020) which stated that, the behavior of a complete pipe support system can often be sufficiently captured using a simplified single-storey frame model. The column is constructed using a 152 mm × 152 mm I-beam and serves as the attachment point for the reinforced beam. A base plate anchors the column during testing. Additional stiffener plates were installed between the bolt holes and the base plate to prevent localized failure and minimize distortion of test results.

The reinforced beam, measuring 100 mm × 100 mm, is fabricated from three welded plates. Stiffener reinforcements were welded on both sides of the beam and connected to the top flange, web, and bottom flange. Endplates were installed at both ends of the beam to facilitate bolted connections to the column.

Mild steel was selected as the material for all components due to its wide availability and common use in structural applications. The material properties used in this study include a Young's modulus of 200 GPa and a yield strength of 250 MPa.

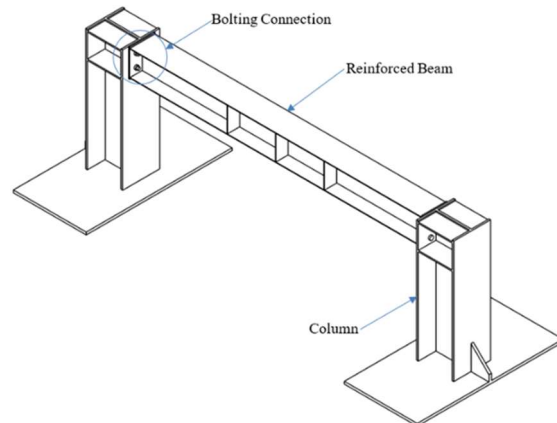


Fig. 1. Model of pipe support with stiffener reinforcement

2.2 Testing Setup and Procedures

To collect stress data, strain gauges (SGs) were attached to the reinforced beam at various locations. For SG1 and SG2 on the top flange, SG3 and SG4 on the web section, and SG5 and SG6 on the bottom flange. The strain gauge layout is shown in Fig. 2. After installation, the pipe support was mounted on the test rig.

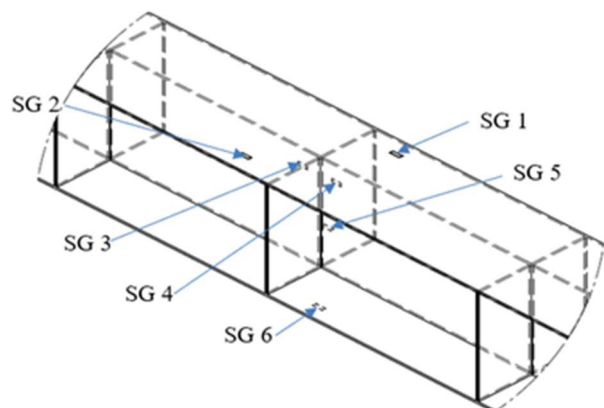


Fig. 2. Location of SG on reinforced beam of pipe support

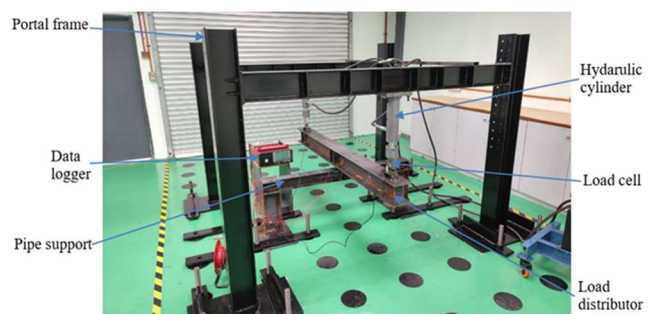


Fig. 3. Concentrated load test setup

In this testing, two load cells were calibrated by SIRIM QAS to ensure the measurement accuracy of applied load. According to calibration certificate, which was published by SIRIM QAS with certificate number of SST/SA/R/2025C/1303 and SST/SA/R/2025C/1304, each

load cell has measurement uncertainty of 52 N. Load cells were placed between hydraulic cylinders and the load distributor to measure the applied force. Bolted connections ensured accurate load transfer. The complete test setup is shown in Fig. 3.

Testing was conducted under static loading conditions. Measurements of load and strain were recorded at 1,000 N intervals. Loading continued until failure of the pipe support occurred. The weight of the load distributor was also considered part of the total applied load, as it was transferred to the pipe support upon contact. In addition, concentrated testing was conducted 3 times to verify the load and stress measurement of concentrated load test was accurately captured.

Stress values were derived from the strain gauge data. For analysis, symmetrical readings from paired gauges (SG1–SG2, SG3–SG4, SG5–SG6) were averaged for the top flange, web, and bottom flange, respectively from the three testing which was conducted.



Fig. 4. Condition of pipe support with stiffener reinforcement after testing

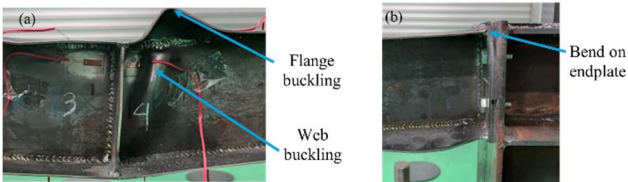


Fig. 5. Failure on pipe support with stiffener reinforcement (a) buckling and (b) bend on endplate

2.3 Result of Concentrated Load Test

For this study, the concentrated load test was carried out until structural failure of the pipe support occurred. Fig. 4 illustrates the overall condition of the pipe support with stiffener reinforcement after testing. Local buckling was observed in the web section and the top flange adjacent to the center stiffener at the load application point. This indicates that the central stiffener effectively enhanced the stiffness of beam, causing the load to be redistributed toward the weaker regions of the beam. In contrast, bending of the endplate was observed as a result of compressive load propagating from the beam ends toward the center along the top flange. The localized buckling represents a local failure mode, while the endplate deformation corresponds to a global structural response, illustrating how the stiffened beam redistributed load between local and global

components during concentrated loading. This distinction highlights the role of stiffener in modifying failure progression within the structure. The buckling and bend failure of pipe support with stiffener reinforcement can be seen in Fig 5.

The stress result from concentrated load test of pipe support with stiffener reinforcement was evaluated using strain gauge at top flange, web, and bottom flange of the reinforced beam. Fig. 6. shows the three repeated results of load tests conducted on each section, the top flange and web of beam experienced compressive stress, while bottom flange experienced tensile stress. In the concentrated load test results, the observed stress exhibited non-linear behavior when the applied load exceeded 25,000 N. Only the stress within the linear region was considered in this study as a comparison with the FEA results. The standard deviation of each section was calculated when the load of 25,000 N to confirm the consistency of result across the load test. Then, it produced the value of 29.7 MPa on top flange, 13.6 MPa on web section, and 1.7 MPa on bottom flange. After that, the average stress result of each section would be used to validate the finite element model of pipe support that can be seen in Fig. 7

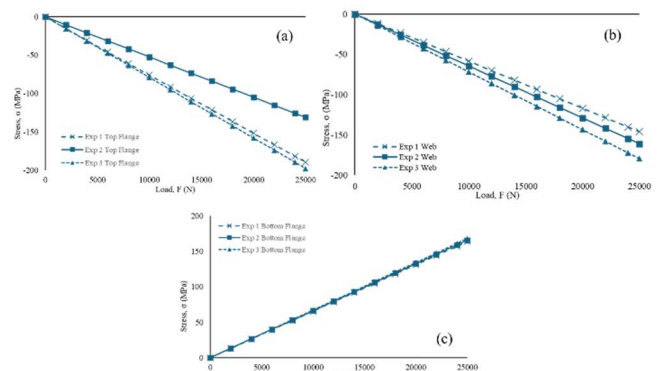


Fig. 6. Three repeated load test results of each section (a) top flange, (b) web, (c) bottom flange

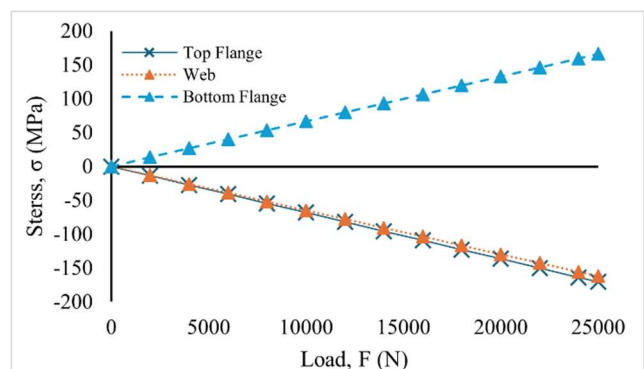


Fig. 7. Average stress-load plot of concentrated load test

3. VALIDATION OF FINITE ELEMENT MODEL

3.1 Pipe Support Modelling

The finite element model of pipe support had been developed using ANSYS software. The loading and boundary condition was adopted according to the conditions of concentrated loading test. Fig. 8 shows the fixed support was employed as an anchorage at baseplate of column. In addition, the loading condition was determined at the center of the beam. It was selected to avoid altered results if the load is applied directly on the top flange of the pipe support beam.

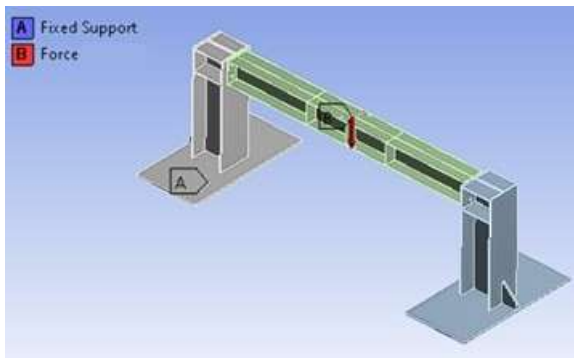


Fig. 8. Finite element model of pipe support with stiffener reinforcement

To represent the actual beam-to-column connection, the contact model between the endplate and column was defined. In this research, the contact body was designated as the column, while the target body was the endplate of the beam. Figs. 9(a) and 9(b) show two distinct connection models that were employed, bonded and frictionless contact.

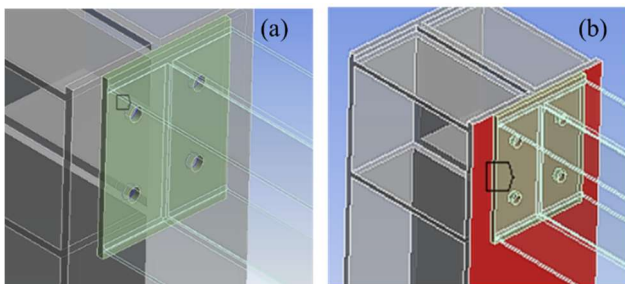


Fig. 9. Connection models (a) bonded contact, (b) frictionless contact

For the bolt holes at the endplate and column interface, a bonded contact formulation was applied between the contact and target bodies. Bonded contact constrains the relative motion between the two surfaces, thereby preventing both separation and sliding. This formulation effectively enforces a fully rigid connection at the interface, enabling the transfer of both normal and tangential forces. In this context, the bonded contact serves as a surrogate representation of the bolted connection, simplifying the numerical model without compromising the overall stiffness behavior.

Meanwhile, frictionless contact was applied to model the

interaction between the surfaces of the endplate and the column flange. This contact type allows the two surfaces to separate or slide freely relative to each other but does not permit penetration. Since no friction is considered, no shear force is transferred across the interface. This approach provides a more realistic simulation of the bearing surface interaction, where only normal contact forces are transmitted between the endplate and the column.

3.2 Comparison Between Result of Finite Element Model and Concentrated Load Test

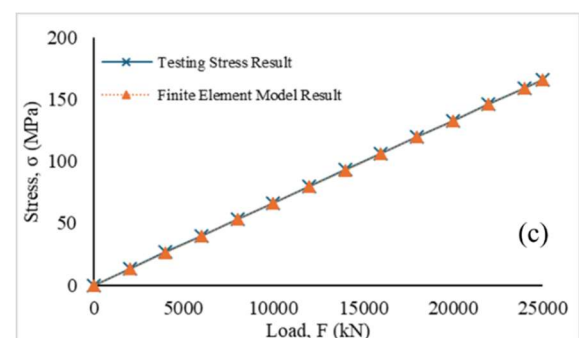
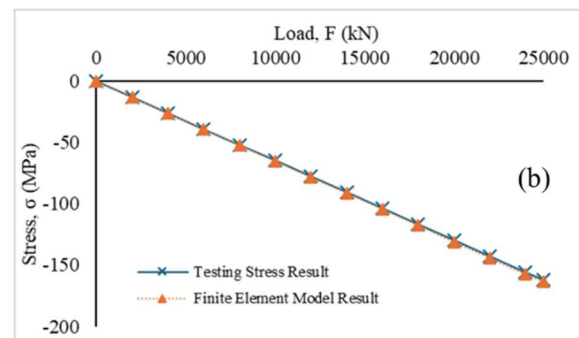
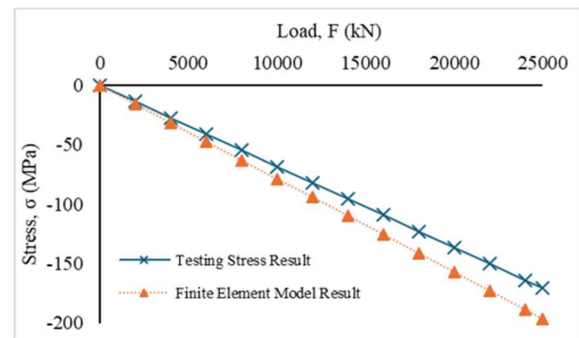


Fig. 10. Stress load plot at (a) top flange, (b) web, (c) bottom flange

The accuracy of the finite element model was assessed by comparing the simulation results with those obtained from the concentrated load test. As shown in the stress–load plots in Figs. 10(a), 10(b), and 10(c), there was strong agreement between the experimental and numerical data across all three sections of the beam: the top flange, web, and bottom

flange.

For comparison, finite element model of pipe support was used solid element with mesh size of 20 mm, produced 58,070 nodes and 26,939 elements. Frictionless contact was used to model the interaction between surfaces of endplate and column. Meanwhile, bonded contact was applied to represent bolting connection on hole of endplate and column. The comparison revealed an overall model accuracy of 94.6%, confirming that the FE model reliably captured the stress behavior of the pipe support under concentrated loading. This validated model was then employed to investigate the relationship between stiffener configurations and load capacity.

3.3 Mesh Convergence

The mesh size used in finite element analysis can significantly influence the accuracy of the results. To ensure mesh independence, a mesh convergence study was conducted following the approach outlined by (Ahmad et al., 2013). The convergence criterion was set at a 5% variation in stress results, consistent with recommendations from Patil and Jeyakarthykeyan (2018) and Azman et al. (2025). Other than that, the displacement of pipe support was also checked and produced similar displacement result around 2.6 mm. As shown in Fig. 11, the stress values stabilized beyond a certain number of mesh element indicating convergence. Therefore, the selected mesh size was deemed adequate, and the results were considered reliable.

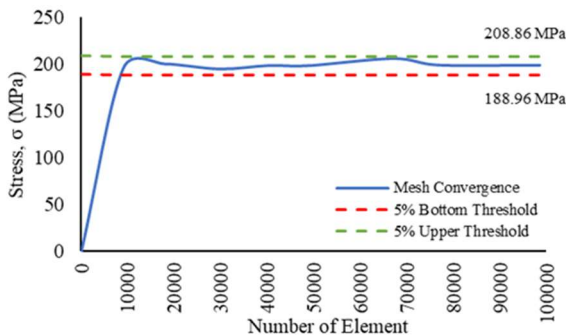


Fig. 11. Mesh convergence study

4. ESTABLISHMENT THE CORRELATION BETWEEN STIFFENER CONFIGURATIONS AND LOAD CAPACITY

This section examines the correlation between various stiffener parameters and the load capacity of pipe support beams. Three parameters were evaluated, beam size, stiffener spacing, and the ratio of stiffener thickness to web thickness (t_s/t_w). A probe point was defined at the center edge of the top flange which identified as a region of high stress under concentrated loading and was used as a reference for all evaluations. The allowable load capacity was determined using a safety factor of 1.5, in accordance

with EN 1990 (2002) and Poutanen et al. (2021).

4.1 Influence of Reinforced Beam Size

The first parameter evaluated was the size of the reinforced beam. The beam was modelled as an I-section with a single stiffener plate located at the center, as shown in Fig. 12. Various nominal I-beam sizes ranging from 8 inches to 24 inches were selected to represent standard structural profiles commonly used in construction. Each beam had a total length of 6 meters, consistent with the maximum length typically used in pipe support applications. To facilitate fair comparison across different beam sizes, normalized load capacity values (load capacity divided by cross-section area, F_c/a) were calculated. This normalization enables direct comparison of structural efficiency among beams with varying sizes. The normalized load capacity demonstrated that geometric size influences overall performance of beam with stiffener reinforcement. The specifications and load capacity for each I-beam size are listed in Table 1.

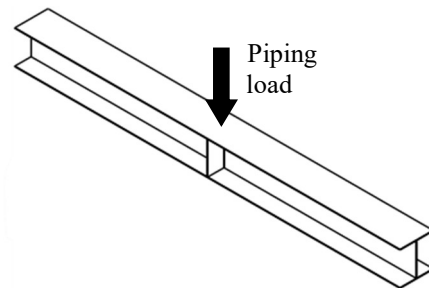


Fig. 12. Reinforced beam model with single stiffener

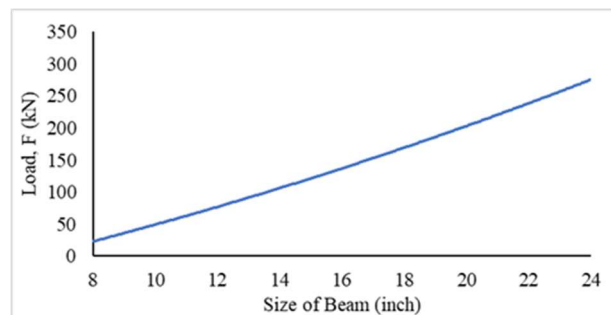


Fig. 13. Load capacity of different reinforced beam

The FEA results for each I-beam size are summarized in Fig. 13, which illustrates the relationship between different reinforced beam size and load capacity. This indicates that larger beam size can withstand higher loads and exhibit greater structural efficiency. The observed increase in load capacity highlights a size effect, where load-carrying capacity grows align with increasing the nominal I-beam size. These results provided the baseline for subsequent evaluations of stiffener spacing and thickness.

4.2 Influence of Stiffener Spacing

Table 1. Specification and load capacity of different beam size

Nominal beam size	Height, h (mm)	Base, b (mm)	Web thickness, t_w (mm)	Flange thickness, t_f (mm)	Load capacity, F_c (kN)	Cross-section area, a (mm ²)	Normalized load capacity, F_n (kN)
8	203.2	133.2	5.7	7.8	32.2	4.7	6.8
12	321.7	102.4	6.6	10.8	67.1	6.7	9.9
16	406.6	143.3	7.9	12.9	115.5	9.9	11.6
20	533.1	209.3	10.1	15.6	230.7	15.9	14.5
24	607.4	179.2	11.3	17.2	281.1	17.6	15.9

Table 2. Thickness of stiffener for different beam size

Nominal beam size	Web thickness, t_w (mm)	Stiffener thickness, t_s (mm)		
		Ratio		
		$t_s / t_w = 1$	$t_s / t_w = 1.5$	$t_s / t_w = 2$
8	5.7	6	9	12
12	6.6	7	11	14
16	7.9	8	12	16
20	10.1	10	15	20
24	11.3	11	17	22

The second parameter evaluated was stiffener spacing. As shown in Fig. 14, multiple stiffeners were modelled along the length of the beam at various intervals (d). The distances considered in this study were 100 mm, 200 mm, 300 mm, and 400 mm. To isolate the effect of spacing, the stiffener-to-web thickness ratio was held constant at $t_s/t_w = 1$ throughout the analysis.

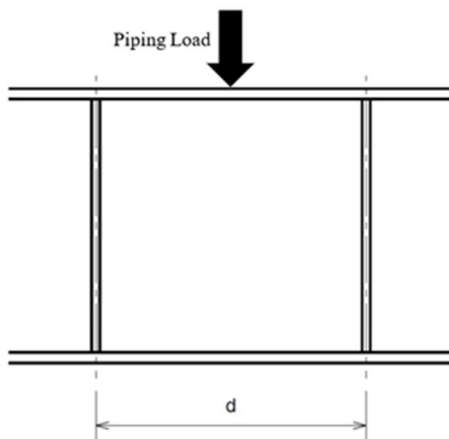


Fig. 14. Stiffener distance for reinforced beam

4.3 Influence of Stiffener to Web Thickness Ratio

The final parameter examined was the ratio of stiffener thickness (t_s) to web thickness (t_w), with consideration for the availability of standard plate sizes in the market. Three values were studied: $t_s/t_w = 1, 1.5,$ and 2 . The actual plate thicknesses corresponding to these ratios for each I-beam size are listed in Table 2.

5. RESULTS AND DISCUSSION

5.1 Influence of Stiffener Distance

The FEA results demonstrated that stiffener distance exerted a significant influence on the load-bearing capacity of pipe support systems, particularly in larger I-beam size. For nominal I-beam size of 8–16 inch, variations in stiffener distance resulted around 2% difference in load capacity. These values are negligible changes in load capacity, indicating that these members possess sufficient load capacity to withstand the applied load regardless of stiffener configuration.

Conversely, for nominal I-beam sizes ranging from 18 to 24 inches, the effect of stiffener distance was more pronounced. Increasing the stiffener distance to 100 mm resulted in approximately a 15% reduction in load capacity, while a distance of 200 mm caused a decrease of around 35%. This indicates a reduced ability of the structure to effectively resist the applied loads as the distance increases. These findings are consistent with the observations reported by Chacón et al. (2013), who demonstrated that shorter stiffener distance enhances the load-bearing capacity of beams subjected to patch loading, by providing improved lateral restraint and delaying local buckling. Similarly, (Kuznetsov and Ponyavina, 2020) highlighted that decreasing stiffener distance contributes to improved overall structural stability under distributed loading condition.

A comparison between the present study and previous research confirms that stiffener distance significantly influences beam load capacity under various loading types, including patch and distributed loads. Concentrated loads induce highly localized stress fields that are more sensitive to stiffener distance than those generated by uniformly distributed loads. Consequently, stiffener configurations for beams subjected to concentrated loading should prioritize reduced distance to effectively delay local buckling and

enhance overall structural stiffness.

Other than that, further increases in stiffener distance beyond 200 mm, in particular distance of 300 mm and 400 mm only showed limited reductions in load capacity roughly 1%–2%. This observation indicates the presence of a threshold beyond which further increments in stiffener distance have a negligible effect on structural load capacity.

As illustrated in Fig. 15, these findings underscore the critical function of stiffener distance in determining the load capacity of pipe supports, particularly for nominal I-beam sizes of 18–24 inch. While nominal I-beam size of 8–16 inch maintained relatively consistent load capacity across a range of stiffener configurations, larger beams exhibited a marked decline in load resistance with increasing stiffener distance up to a certain limit. This study extends these findings by identifying a stiffener distance threshold of approximately 200 mm under concentrated load, providing a practical reference for the design of pipe support with stiffener reinforcement.

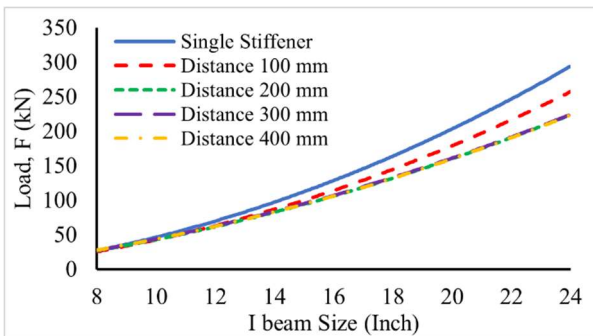


Fig. 15. Influence of stiffener distance on load capacity for different I-beam sizes

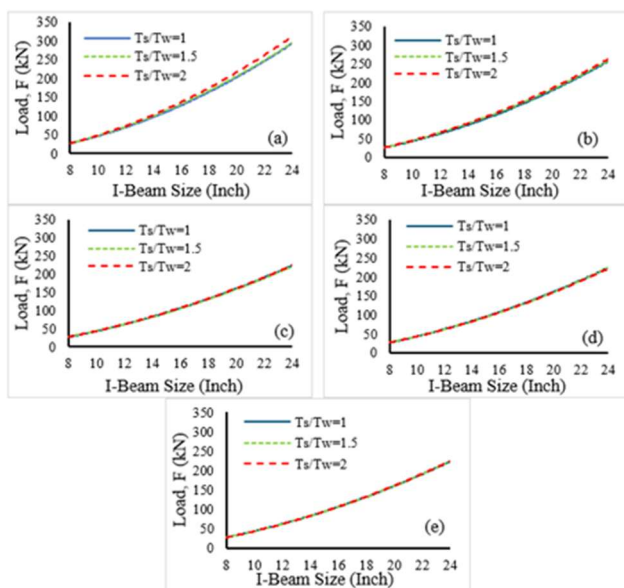


Fig. 16. Influence of stiffener thickness on load capacity for different I-beam size with (a) single stiffener, (b) 100 mm distance, (c) 200 mm distance, (d) 300 mm distance, and (e) 400 mm distance

5.2 Influence of Stiffener Thickness

Following the investigation of stiffener distance, the influence of stiffener thickness on load capacity was subsequently evaluated. FEA was employed to assess the load capacity of beams reinforced with both single and multiple stiffeners. For the multi-stiffener configurations, stiffener distance was set at 100, 200, 300, and 400 mm.

In this study found that stiffener thickness generally had a limited impact on the overall load capacity of the beams. For all other beam sizes, changes in stiffener thickness roughly about 1% and did not significantly affect structural performance. Similarly, in beams reinforced with multiple stiffeners over the specified distance intervals, increasing the stiffener thickness also did not lead to any notable increase or decrease in load capacity.

A comprehensive comparison of load capacities across different beam sizes and stiffener thicknesses for both single- and multi-stiffener configurations is presented in Figs. 16(a) to 16(e). These findings emphasize the limited structural benefit of increasing stiffener thickness and provide critical insights for the efficient design of stiffener-reinforced pipe supports, guiding material optimization in structural reinforcement applications.

5.3 Recommendation for Stiffener Configuration Based on Configuration

From the data of load capacity from different parameters, it might be used as guideline to decide stiffener configuration for pipe support beam. For stiffener thickness, only ratio $t_s/t_w = 1$ was provided because stiffener-to-web thickness 1.5 and 2 had negligible effect to the load capacity of beam. Also, stiffener distance would be offered with distance of 100 and 200 mm. The distance of 300 and 400 mm was excluded because there was no more influence on load capacity when the stiffener distance more than 200 mm.

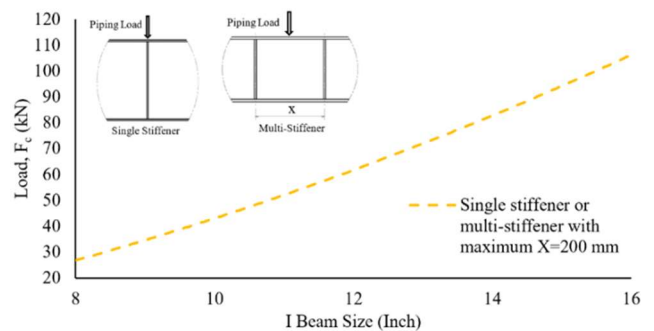


Fig. 17. Correlation between load capacity and stiffener parameters for nominal beam size 8–16 inch

For small beam size with nominal range of 8-inch to 16-inch, the inclusion of 100 and 200 mm stiffener distance on load capacity was found to be limited effect compared to single stiffener configuration. Thus, the stiffener configuration could be applied for small beam size of pipe

support subjected to concentrated load was single stiffener or multi-stiffener with maximum stiffener distance of 200 mm. The correlation between load capacity and stiffener parameters for nominal beam size of 8–16 inch can be seen in Fig. 17.

For the nominal beam size which is bigger than 16-inch, the influence of stiffener distance on load capacity was more significant. When the stiffener distance was increased to 100 mm, the load capacity decreased around 15%. Further increasing the distance to 200 mm resulted in reduction of load capacity up to 35% compared to single stiffener configuration. It shows that the single stiffener is the most suitable configuration for larger nominal beam size to withstand high load capacity compared to the stiffener with distance of 200 mm. The correlation between load capacity and stiffener parameters for nominal beam size of 18–24 inch is presented in Fig. 18.

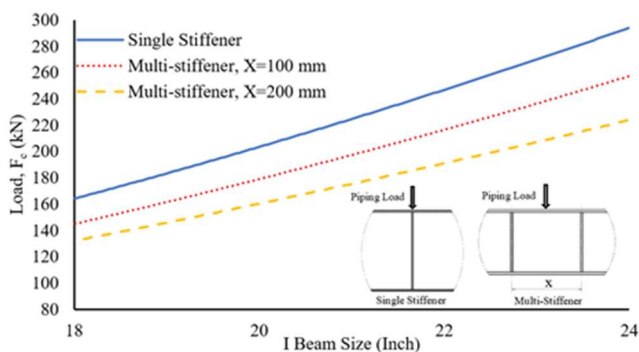


Fig. 18. Correlation between load capacity and stiffener parameters for nominal beam size of 18–24 inch

According to the correlation between load capacity and stiffener parameters, it produced a guideline which can be implemented in industries that use pipe support. The guideline can be used to define stiffener configurations to increase the load capacity of pipe support subjected to the concentrated load. For the nominal beam size of 8 to 16 inch, the stiffener configuration can be single or multi-stiffener with maximum distance of 200 mm and 1:1 thickness ratio. Meanwhile, for nominal beam size of 18 to 24 inch, the stiffener configuration can be applied according to the required load with thickness ratio can be maintained at 1:1. Single stiffener configuration has the highest load capacity subjected to the concentrated load. If the required load is 15% less than the capacity of single stiffener, multi-stiffener with 100 mm distance can be applied. Furthermore, if the load is 35% less than the capacity of single stiffener, multi-stiffener with 200 mm distance can be used for the pipe support.

6. CONCLUSION

This study established a correlation between stiffener configurations and the load capacity of pipe support beams through both concentrated testing and FEA. This research specifically discusses the main technical challenges

associated with the lack of guidelines on the design and configuration of stiffener reinforcement on pipe support structures.

The following conclusions are drawn:

- (1) The validated model achieved an overall accuracy of 94.6%, confirming its capability to capture realistic stress behavior under concentrated loading.
- (2) Beam size significantly influences load capacity, with larger beams exhibiting higher load capacity that can be withstand by the pipe support.
- (3) Stiffener distance has a pronounced impact on load capacity of pipe support. Increasing the distance to 100 mm or 200 mm reduces structural load capacity, while increases beyond 200 mm showed no further reduction of load capacity.
- (4) Stiffener thickness has only a limited effect on load capacity. As such, increasing thickness beyond a t_s/t_w ratio of 1 offers negligible structural advantage. Thus, a 1:1 thickness ratio is sufficient without compromising the load capacity of the pipe support.
- (5) A design guideline of stiffener configuration is provided, for nominal beam size of 8 to 16 inch, either single stiffeners or multiple stiffeners spaced up to 200 mm are recommended. For beam size of 18 to 24 inch, a single stiffener provides superior load capacity and structural efficiency. On the other hand, the load capacity will decrease about 15% if the stiffener distance increase to 100 mm and 35% if the stiffener distance increase to 200 mm.

These findings contribute to provide design guidelines of stiffener configuration for the engineers and can be implemented in industrial practices which use the pipe support or similar structures.

DECLARATION OF COMPETING INTEREST

All authors have read and approved the manuscript, and there are no conflicts of interest to declare.

DATA AVAILABILITY

The data supporting the findings of this study, including stress result and FEA input files are available from the corresponding author upon reasonable request.

ACKNOWLEDGMENT

In this journal, correlation between stiffener configurations and load capacity for pipe support beam is evaluated in the framework of a research study at Faculty of Mechanical Technology and Engineering, Universiti Teknikal Malaysia Melaka (UTeM). The authors would like to express gratitude to the Applied Mechanical Design Laboratory for providing the facility. The authors gratefully acknowledge UTeM and Kesidang Scholarship for

providing access to open access articles which supported this research.

REFERENCES

- Ahmad, M., Ismail, K.A., Mat, F. 2013. Convergence of finite element model for crushing of a conical thin-walled tube. *Procedia Engineering*, 53, 586–593.
- Alinia, M.M. 2005. A study into optimization of stiffeners in plates subjected to shear loading. *Thin-Walled Structures*, 43, 845–860.
- Alshoabi, A.M. 2015. An adaptive finite element framework for fatigue crack propagation under constant amplitude loading. *International Journal of Applied Science and Engineering*, 13, 261–270.
- Azman, A.N.N., Venkatason, K., Sivaguru, S. 2025. Mesh convergence analysis on the aerodynamic performance of a sedan vehicle. *Journal of Engineering Technology and Applied Physics*, 7, 85–95.
- Basiński, W. 2019. Design of transverse stiffeners in plate girders with corrugated web. *Periodica Polytechnica Civil Engineering*, 63, 577–592.
- Bougoffa, S., Durif, S., Mezghanni, O., Bouchaïr, A., Daoud, A. 2023. Analysis of beam web panels with full length transverse stiffener in Compression. *Engineering Structures*, 297, 116996.
- Chacón, R., Mirambell, E., Real, E. 2013. Transversally stiffened plate girders subjected to patch loading. Part 1. Preliminary Study. *Journal of Constructional Steel Research*, 80, 483–491.
- Chen, C.-H., Ou, C.-I. 2009. Modal identification from field test and FEM updating of a long span cable-stayed bridge. *International Journal of Applied Science and Engineering*, 6, 251–262.
- Choi, B.H., Kang, Y.J., Yoo, C.H. 2007. Stiffness requirements for transverse stiffeners of compression panels. *Engineering Structures*, 29, 2087–2096.
- Drake, R.M., Walter, R.J. 2010. Design of structural steel pipe racks. *Engineering Journal, American Institute of Steel Construction*, 47, 241–252.
- EN 1990. 2002. Eurocode - Basis of structural design.
- Gavare, P.R., Patil, S.N. 2018. Parametric study of plate girder using different stiffener arrangement. *International Journal of Advanced Research in Science and Engineering*, 7, 1161–1174.
- Gupta, H., Sathe, R.S., Sharma, J.K. 2022. Numerical analysis on load-settlement response of reinforced granular blanket over ordinary stone column. *International Journal of Applied Science and Engineering*, 19, 2022057.
- Huang, Z., Tian, Y., Zhang, Y., Shi, T., Xia, Q. 2024. Buckling optimization of curved grid stiffeners through the Level Set Based Density Method. *CMES - Computer Modeling in Engineering and Sciences*, 140, 711–733.
- Kawade, M. G., Navale, A.V. 2019. Optimization of pipe rack by study of braced bay. *International Journal of Research in Engineering, Science and Management*, 2, 451–455.
- Kurepatil, R.Y., Patil, S.K., Pujari, A.B. 2024. Study of pipe rack design under different support conditions. *International Journal of All Research Education and Scientific Methods (IJARESM)*, 12, 137–140.
- Kuznetsov, D.N., Ponyavina, N.A. 2020. Numerical study of the influence of the distance between stiffeners on the loss of stability of the web of an i-section steel beam. *IOP Conference Series: Materials Science and Engineering*, 753, 042041.
- Lee, J.-S., Shin, K.-J., Woo, J.-H. 2024. Experimental and analytical study on non-damaged reinforcement method for pipe rack steel structures. *Buildings*, 14, 2637.
- Maiorana, E., Pellegrino, C., Modena, C. 2011. Influence of longitudinal stiffeners on elastic stability of girder webs. *Journal of Constructional Steel Research*, 67, 51–64.
- Meshram, P.D., Prasad, R.K. 2021. Design of optimum pipe rack for various bays. *International Research Journal of Modernization in Engineering Technology and Science*, 3, 1935–1944.
- Nagdeote, R.D., Suryawanshi, S.R., Khadake, N. 2021. A review on optimization in design and construction of pipe supports, pipe frames and T posts. *International Research Journal of Engineering and Technology*, 8, 722.
- Nerenst, T.B., Ebro, M., Nielsen, M., Eifler, T., Nielsen, K.L. 2021. Exploring Barriers for The Use of FEA-Based Variation Simulation in Industrial Development Practice. *Design Science*, 7, Article e21.
- Papazafeiropoulos, G., Vu, Q.-V., Nguyen, V.-S., Truong, V.-H. 2022. Optimum location of a single longitudinal stiffener with various cross-section shapes of steel plate girders under bending loading. *Journal of Science and Technology in Civil Engineering (STCE) - HUCE*, 16, 65–75.
- Patil, H., Jeyakarthykeyan, P.V. 2018. Mesh Convergence Study and Estimation of Discretization Error of Hub in Clutch Disc with Integration of ANSYS. *IOP Conference Series: Materials Science and Engineering*, 402, 012065.
- Peng, Y., Kong, Z., Dinh, B.H., Nguyen, H.H., Cao, T.S., Papazafeiropoulos, G., Vu, Q.V. 2023. Web Bend-Buckling of Steel Plate Girders Reinforced by Two Longitudinal Stiffeners with Various Cross-Section Shapes. *Metals*, 13, 323.
- Plevris, V., Markeset, G. 2018. Educational challenges in computer-based finite element analysis and design of structures. *Journal of Computer Science*, 14, 1351–1362.
- Poutanen, T., Lämsivaara, T., Pursiainen, S., Mäkinen, J., Asp, O. 2021. Calculation of safety factors of the eurocodes. *Applied Sciences (Switzerland)*, 11, 1–9.
- Shah, S.M.I., Ganesh, G.M. 2022. Impact of diameter to thickness (D/t) on axial capacity of circular CFST

- columns: Experimental, parametric and numerical analysis. *International Journal of Applied Science and Engineering*, 19, 2021486.
- Sholikhah, M., Ridwan, R., Prabowo, A.R., Ghanbari-Ghazijahani, T., Yaningsih, I., Muhayat, N., Tjahjana, D.D.D.P., Adiputra, R., Sohn, J.M. 2024. strength assessment of stiffened-panel structures against buckling loads: FE benchmarking and analysis. *Civil Engineering Journal (Iran)*, 10, 1034–1050.
- Sinur, F., Beg, D. 2012. Intermediate transverse stiffeners in plate girders. *Steel Construction*, 5, 23–32.
- Tsavdaridis, K.D., Galiatsatos, G. 2015. Assessment of cellular beams with transverse stiffeners and closely spaced web openings. *Thin-Walled Structures*, 94, 636–650.
- Wang, S., Zhang, H. 2023. A New Design Method for Stiffened Plate Based on Topology Optimization with Min-Max Length-Scale Control. *Frontiers in Materials*, 10, 1277421.
- Yussof, M.M., Silalahi, J.H., Kamarudin, M.K., Chen, P.S., Parke, G.A.R. 2020. Numerical Evaluation of Dynamic Responses of Steel Frame Structures with Different Types of Haunch Connection under Blast Load. *Applied Sciences (Switzerland)*, 10, 1815.
- Zhang, G., Hu, Y., Yan, B., Tong, M., Wang, F. 2024. Buckling and Post-Buckling Analysis of Composite Stiffened Panels: A Ten-Year Review (2014–2023). *Thin-Walled Structures*, 205, 112525.